Korean J. Chem. Eng., 34(4), 977-986 (2017)
DOI: 10.1007/s11814-016-0367-0

pISSN: 0256-1115
eISSN: 1975-7220

Prediction of the self-diffusion coefficients in aqueous KCl solution using molecular dynamics: A comparative study of two force fields

Mohammad Amin Esmaeilbeig and Salman Movahedirad†

School of Chemical Engineering, Iran University of Science and Technology (IUST), Tehran, Iran
(*Received 31 October 2016 • accepted 29 December 2016*)

Abstract−Molecular dynamic simulation was used to calculate the self-diffusion coefficients of ions in aqueous KCl solution. The simulations were performed for enough time (12 ns) in the form of all-atom to determine the accurate values of the self-diffusion coefficients. The values of the self-diffusion coefficients were calculated by Einstein equation. Two different force fields of Dang and Deublein were employed in the simulations, and we found that at low ion concentration (equal or less than 3 mol/(kg of H_2O)), the Dang force field is more accurate for prediction of the self-diffusion coefficient of K^+ ions and Deublein force field is more accurate for Cl^- ions. An Arrhenius type equation was used to model the temperature dependence of the self-diffusion coefficients and the diffusion activation energies at different ion concentrations were reported.

Keywords: Self-diffusion Coefficient, Molecular Dynamics, Einstein's Method

INTRODUCTION

Aqueous electrolyte solutions are very important in biological, chemical and environmental processes [1-3]. Water is a strongly polar liquid and the presence of charged ions in the water medium can affect the mobility of water molecules. The physical behavior of aqueous electrolyte solutions depends on water-ion interaction. One of these solutions is aqueous KCl solution in which the K^+ and Cl^- ions are dispersed in the liquid medium. This aqueous electrolyte solution is used in electrochemical capacitors [4]. In addition, this electrolyte contains important ions for human body [5]. Some of the recent works in usage of KCl electrolytes are available in the literature [6,7]. One such work, published by Kim et al., is about the effect of KCl electrolyte on the electrochemical behavior of electric double layer capacitors based on a porous silicon carbide electrode [7].

Molecular movement in the fluid medium is significant and affects the bulk properties of material such as their transport properties. To design, control and optimize any chemical process, the transport properties play important roles. Rheological, thermal and molecular diffusion behaviors for many fluids have been investigated broadly in literature [8-10]. These properties are related to the molecular behavior of a fluid. Thus, the study of molecular behavior of any material can lead to the calculation of these properties [11]. One of these properties is the self-diffusion coefficient, which shows the mobility of molecules in a mixture. The self-diffusion coefficient shows the diffusion of a species in the absence of a driving force and is related to the Brownian motion of that species.

The measurement of the self-diffusion coefficients of materials is not straightforward because determination of diffusion flux of one component in the medium of the same component is infeasible [9]. Some of the methods for the measurement of self-diffusion coefficients are nuclear magnetic resonance (NMR) [13], neutron diffraction [14] and radioisotopic methods [15]. Furthermore, some theoretical models have been developed to predict the self-diffusion coefficient [16,17]. Molecular simulation is a strong tool for calculation of the self-diffusion coefficient. Some of the recent works on the calculation of the self-diffusion coefficients by molecular dynamic (MD) simulation are available in literature [18-20].

Molecular simulation methods are useful for calculation of material properties and prediction of chemical phenomena. Using this tool, those properties of materials for which their measurement is expensive, can be predicted. Moreover, some phenomena for which their experimental study is difficult, can be simulated in computational space. These simulations consist of different methods, such as molecular dynamics (MD) and Monte Carlo (MC) [21]. In MD, governing equations are based on classical Newtonian mechanics and the particle positions in each time step can be calculated by the aid of these equations.

In molecular dynamics, the systems are simulated in the forms of all-atoms or coarse-grain. In the all-atoms type, each atom in a molecule is considered as an interaction site, while in the coarse-grain model different atoms are grouped in a single interaction site named "pseudo-atom." Thus, in the coarse grain method, the speed of simulation is higher than in all-atom one. The MD method can be used in simulation of electrolyte systems. Some of the recent works on MD simulations of electrolyte solutions can be found in references [22-26].

In the present work, the KCl aqueous electrolyte solution was simulated in the form of all-atom by molecular dynamics simulation approach. The simulations were performed by using two different force fields for ions. The self-diffusion coefficients of ions over the temperature range of 280-340 K and ion molality between 1.13-6.17 mol/kg H_2O, were calculated.

†To whom correspondence should be addressed.
E-mail: movahedirad@iust.ac.ir

METHODOLOGY

1. Theoretical Background

For calculation of transport properties by molecular dynamic simulation, there are two approaches: non-equilibrium molecular dynamics (NEMD) and equilibrium molecular dynamics (EMD) [27]. Calculating the transport properties by EMD is based on the linear response theory [28]. The correlation functions of microscopic fluxes are naturally decayed in EMD runs and the transport properties can be determined by Green-Kubo formulas [29]. Furthermore, to obtain accurate results from EMD simulations, the simulation should be done for a long time [30] and the integrals of the flux correlation functions over the time converge poorly. On the other hand, interpretation of the NEMD results is difficult due to the problems related to the simulation techniques [27]. In the present work, the EMD method is selected, and the simulations are carried out for sufficiently long time.

In the calculation of self-diffusion coefficients, there are two general methods with specific data. The first method deals with the positions of molecules and the second one deals with their velocities. In the first method, the ensemble average of mean square displacement (MSD) of the molecules is related to the self-diffusion coefficient. This method is called Einstein method [30]. By this method, the self-diffusion coefficient can be calculated according to Eq. (1).

$$D_{ii} = \lim_{t\to\infty} \frac{1}{2dNt} \left\langle \sum_{i=1}^{N} [r_i(t) - r_i(0)]^2 \right\rangle \tag{1}$$

where D_{ii} is the self-diffusion coefficient of specie i, r_i is the center of mass position of the molecule i, N is the total number of molecules, t is the total simulation time and d is the dimensionality of system (e.g., for 2d system d=2). The infinity symbol means that the calculation should be done for sufficiently long time. Hence, if the ensemble average of MSD is plotted versus time, a linear curve is achieved and the slope of this line equals to $2dD_{ii}$. The slope should be calculated for a sufficiently long time. Special care should be taken using the Einstein method for self-diffusion calculation because of applying periodic boundary conditions in the simulations. In the second method, the self-diffusion coefficient is calculated by integrating the ensemble averaged of velocity auto-correlation functions (VACF) of the molecules over the time [30]. This method is called Green-Kubo method (Eq. (2)).

$$D_{ii} = \frac{1}{3N} \int_0^{\infty} \left\langle \sum_{i=1}^{N} v_i(t) v_i(0) \right\rangle dt \tag{2}$$

where v_i denotes the velocity of the molecule "i". In contrast to Einstein equation, in this equation, the time symbol denotes the time step of VACF. The second method is very time consuming [30], and thus the first method is preferable to calculate the self-diffusion coefficient. In the present study, the Einstein method is used.

One of the factors that affect the value of self-diffusion is temperature. Apparently, temperature increment leads to rise in the self-diffusion coefficient. Temperature dependence effect on the self-diffusion could be modeled by Arrhenius type equations (Eq. (3)) [30]. In Eq. (3), D_0 shows the limit of self-diffusion coefficient when the temperature approaches infinity. Moreover, E is the diffusion activation energy [30].

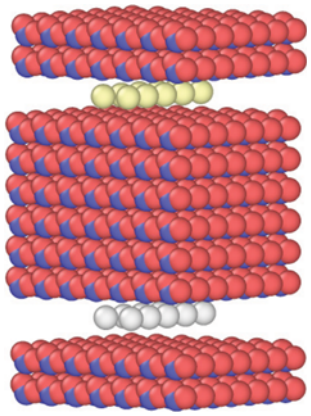

Fig. 1. The initial structure for simulation of aqueous KCl solution. White and yellow particles are ions and the others are water molecules.

$$D = D_0 \exp\left(-\frac{E}{RT}\right) \tag{3}$$

2. Simulation Details

When a halide salt such as KCl is dissolved in a water medium, the ions which are in the lattice structure of halide are separated from each other and disperse in the water medium and make aqueous electrolyte solution. According to this issue, the simulation of this medium should consist of water molecules and separated ions. In this work a cubic box was used to simulate the aqueous solution. In the initial configuration of system, the molecules and ions were arranged layer by layer. One of These arrangements is shown in Fig. 1.

To investigate the total potential energy of the system, the interactions between atoms should be determined. The interactions between atoms are in the forms of bonded and non-bonded interactions. The non-bonded interactions contain van der Waals dispersion interaction and electrostatic Coulombic one. The dispersion interactions were modeled by Lennard-Jones (6-12) relation according to Eq. (4), and electrostatic interactions were modeled by Coulomb's law as stated in Eq. (5). In these equations, r_{ij} is the distance between atoms "i" and "j", ε_{ij} and σ_{ij} are the parameters of energy and distance of interaction in Lennard-Jones model, respectively. q_i and q_j are partial charges of atoms and ε_0 is permittivity in the vacuum.

$$U_{ij}^{LJ} = 4\varepsilon_{ij}\left[\left(\frac{\sigma_{ij}}{r_{ij}}\right)^{12} - \left(\frac{\sigma_{ij}}{r_{ij}}\right)^{6}\right] \tag{4}$$

$$U_{ij}^{Coul} = \frac{q_i q_j}{4\pi\varepsilon_0 r_{ij}} \tag{5}$$

For water molecules, there are many potential force fields such as SPC [31], SPC/E [32], TIP3P [33] and TIP4P [34]. For K^+ and Cl^- ions there are force fields such as Dang [35], Joung & Cheatham [35] and Deublein et al. [36]. The models SPC, SPC/E and TIP3P consider three interaction sites on each water molecule. One of

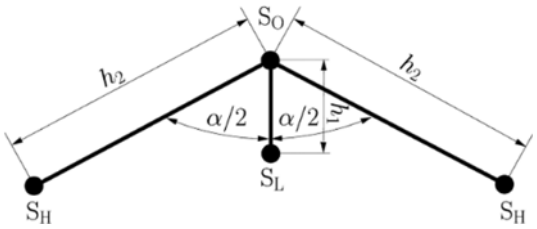

Fig. 2. The geometry of TIP4P model [37].

Table 1. The dimensions of TIP4P model [37]

h_1 (Å)	h_2 (Å)	α (deg)
0.15	0.9572	104.52

Table 2. The partial charges and constants for each model of water molecule [37,38]

Model	Species i	q_i (e)	ε_{ii} (kcal/mol)	σ_{ii} (Å)
SPC	O	−0.82	0.1553	3.166
	H	+0.41	0.0	0.0
SPC/E	O	−0.8476	0.1553	3.166
	H	+0.4238	0.0	0.0
TIP3P	O	−0.83	0.102	3.188
	H	+0.415	0.0	0.0
TIP4P	O	0.0	0.155	3.15365
	H	+0.52	0.0	0.0

these sites is on oxygen atoms and two other sites are on hydrogen atoms. But, the model TIP4P considers four interaction sites on each water molecule. The three interaction sites of this model are the same as other models. The fourth site is placed along the bisector of HOH angle. Fig. 2 illustrates this model, schematically. In this figure, S_H and S_O are the interaction sites on hydrogen and oxygen atoms, respectively. S_L is the fourth site of interaction. The dimensions of this model [37] are listed in Table 1. In all of the models, the interaction type of site on hydrogen atoms is only Coulombic. In TIP4P model the van der Waals interaction is only considered for oxygen atom site. But in the other models the interaction site on the oxygen atoms has both van der Waals and Coulombic interactions. The fourth site of the model TIP4P has only Coulombic interaction and its partial charge equals to −1.04. The magnitude of partial charges and constants of van der Waals interactions are listed in Table 2 [37,38].

In the present study, the interatomic potential used for water molecules was SPC/E force field. The interatomic potential for ions was calculated by two force fields: 1-Dang [35] and 2-Deublein et al. [36]. The Dang interatomic potential was released in 1995, but the Deublein et al. force field was released in 2012. The values of parameters in the force fields of ions are listed in Table 3. The Lorentz-Berthelot mixing rule was used to calculate the energy and length parameters of Lennard-Jones pair function for two different types of atoms:

Table 3. The values of parameters of potential functions for ions

Force field	Species i	q (e)	ε_{ii} (kcal/mol)	σ_{ii} (Å)
Deublein et al. [36]	K^+	+1.0000	0.1987	2.7700
	Cl^-	−1.0000	0.1987	4.4100
Dang [35]	K^+	+1.0000	0.1000	3.3320
	Cl^-	−1.0000	0.1000	4.4010

$$\varepsilon_{ij} = \sqrt{\varepsilon_{ii}\varepsilon_{jj}} \tag{6}$$

$$\sigma_{ij} = \frac{\sigma_{ii} + \sigma_{jj}}{2} \tag{7}$$

The cutoff distance was assumed to be 12 Å for both van der Waals and electrostatic potentials. The long term of electrostatic interactions was modeled by PPPM (particle-particle, particle-mesh) with accuracy of $10^{-3.61}$. The PPPM method is much faster than older methods such as Ewald. In this method, the long range electrostatic interactions are calculated by particle-mesh method [39]. The bond lengths and angles of water molecules were fixed by SHAKE algorithm. This algorithm was used to accelerate the simulations. Because the covalent bond stretching and angle bending are fast motions and these motions determine the time step [40]. If the covalent bond and angle of water molecule are set to fixed quantities, larger time steps could be used.

LAMMPS (Large scale atomic/molecular massively parallel simulator) [41], a free and open source software was used for simulations. Simulations were performed for five different concentrations. The number of water molecules, ions and concentration for each simulation are listed in Table 4. The simulations are at five temperatures ranging from 280 to 340 K. Note that the concentration of K^+ ions equals to concentration of Cl^- ions. In the present work, for each force field, 25 simulations were performed.

The periodic boundary condition was applied to systems in three dimensions. The time step was considered 1fs for every simulation and velocity the Verlet algorithm [39] was used for time integration. The initial velocity of atoms was set based on Gaussian distri-

Table 4. Concentrations and molecular numbers used in simulations

Concentration level	n_{H_2O}	n_{K^+}	n_{Cl^-}	Molality of K^+ (mol K^+/kg H_2O)	Molality of Cl^- (mol Cl^-/kg H_2O)
1	450	50	50	6.173	6.173
2	460	40	40	4.831	4.831
3	470	30	30	3.546	3.546
4	480	20	20	2.315	2.315
5	490	10	10	1.134	1.134

bution with the temperature equals to 700 K. The simulations were performed in five steps. In all steps that the simulation was run in NPT ensemble, the Nose-Hoover thermostat and barostat was used.

- To disperse the ions in the water medium, first the systems were simulated for 1000 time steps in NPT ensemble. The temperature and pressure of this ensemble were set to 700 K and 0.001 bar, respectively. Applying high temperature and low pressure, led to the expansion of the system.
- The system was simulated for 1000 timesteps in the same ensemble with target temperature and a pressure equals to 10 bars to compress the expanded system and reach to the liquid state.
- Equilibration was performed in NPT ensemble with the condition of target temperature and atmospheric pressure. This stage was run for 1500 time steps.
- Then the system was simulated in NVE ensemble for 1000 time steps. The main purpose for this step was to analyze the stability of the simulation [42].
- Finally, the system ran about 12 ns in NPT ensemble with the condition of target temperature and atmospheric pressure.

RESULTS AND DISCUSSION

To analyze the stability of simulation, the variation of parameters of simulation in NVE step should be investigated. Thus, the temperature and potential energy of system were selected. The variations of these two parameters in NVE steps for one of the simulations are plotted in Fig. 3. According to this figure, the variations are negligible and the system is stable. Also, the equilibrium configuration of the water molecules and ions is shown in Fig. 4.

1. Density of Aqueous Solutions

Variations of the aqueous KCl solution density with the salt molality equal 1.134 mol/kg H_2O at 300 K versus time are sketched in Fig. 5. Deublein force field was used for this simulation. In this figure, each mentioned simulation step is demonstrated by a differ-

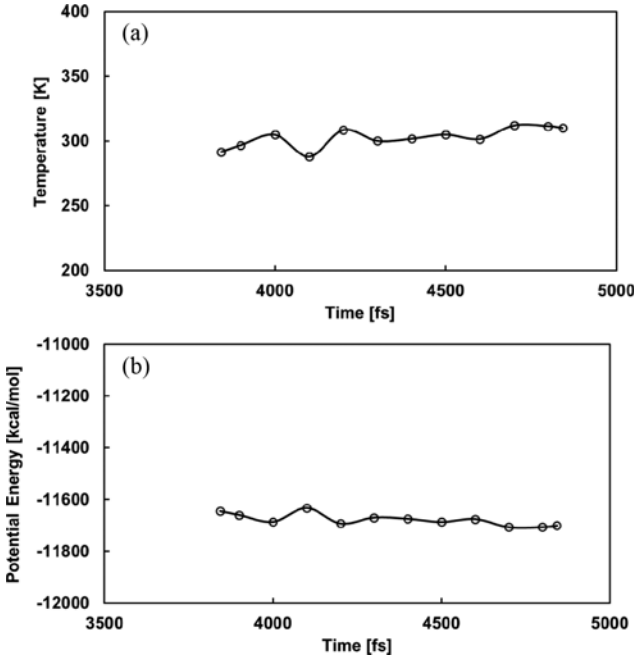

Fig. 3. Variations of (a) temperature and (b) potential energy versus time for simulation in NVE.

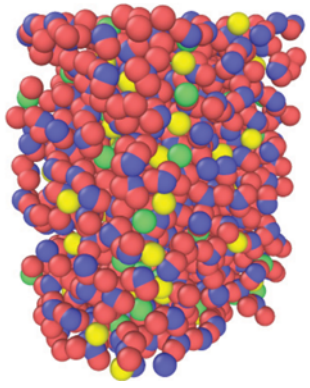

Fig. 4. The configuration of water molecules and ions in equilibrium state. Yellow and green particles are ions.

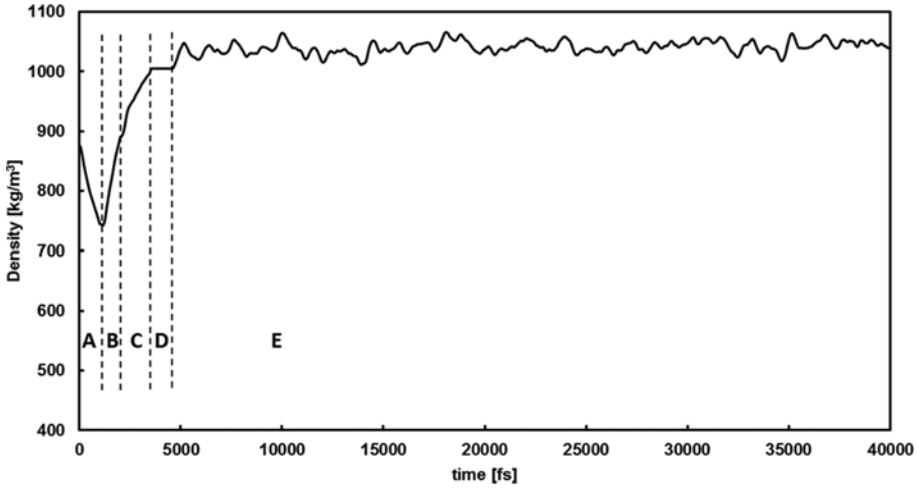

Fig. 5. Density variation of aqueous KCl solution with molality equal to 1.134 mol/kg H_2O at 300 K during the simulation using the Deublein force field. The simulation steps were: (a) Heating; (b) cooling; (c) equilibration; (d) NVE and (e) final step.

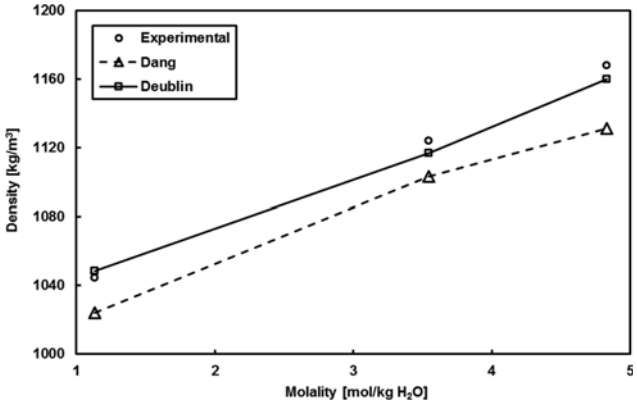

Fig. 6. A comparison between the calculated densities by Dang and Deublein force fields with experimental data [43] at 300 K.

ent letter (A to E). According to this figure, the required simulation time for calculation of density is much lower than one for self-diffusion coefficient. Thus, in the final step of simulation, the density of solution changes with very slightly fluctuations.

The calculated densities for three aqueous solutions with different molality at 300 K using both Deublein and Dang force fields were compared with experimental data [43] as shown in Fig. 6. In comparison with experimental data, the average relative errors for predictions of Deublein and Dang force fields were about 0.58% and 2.32%, respectively. Thus, it can be concluded that for calculating the density of aqueous KCl solution at 300 K and in this range of molality, the Deublein force field will be more accurate than Dang force field model.

2. Radial Pair Distribution Functions

Radial pair distribution function (RDF), which is commonly used for validation of molecular simulation results, gives the average particle number density as a function of distance from arbitrary particles [44]. The structural characteristics of liquid phase can be checked by this function. In electrolyte solutions, generally, there are three types of interactions: water-water, ion-water and ion-ion interactions. In the water-water group, there are three RDFs: O-O, O-H and H-H. In the ion-water group there are four RDFs: K^+-H, K^+-O, Cl^--H and Cl^--O. In the ion-ion group there are three RDFs: K^+-K^+, Cl^--Cl^- and K^+-Cl^-. In the present work, some of above RDFs have been considered and the effects of temperature and ion concentration were investigated.

Fig. 7 shows some RDFs of ion-water type. The first peak of Fig. 7(a) occurs at shorter distance than Fig. 7(b), which is related to the intermolecular forces. According to the types of intermolecular forces that are present in the simulation, the electrostatic force can affect the distance of the first peak. The potassium ions and oxygen atoms have attraction electrostatic force due to opposite charges, but the charges of chloride ions and oxygen atoms are similar. Thus, they repulse each other. The distance between potassium ions and oxygen atoms is shorter due to the attraction forces (Fig. 7(a)). On the other hand, the repulsion force makes the distance between chloride ions and oxygen atoms longer (Fig. 7(b)).

According to Fig. 7, it seems that as the ion concentration in aqueous solution increases, the value of the first peak of the RDF

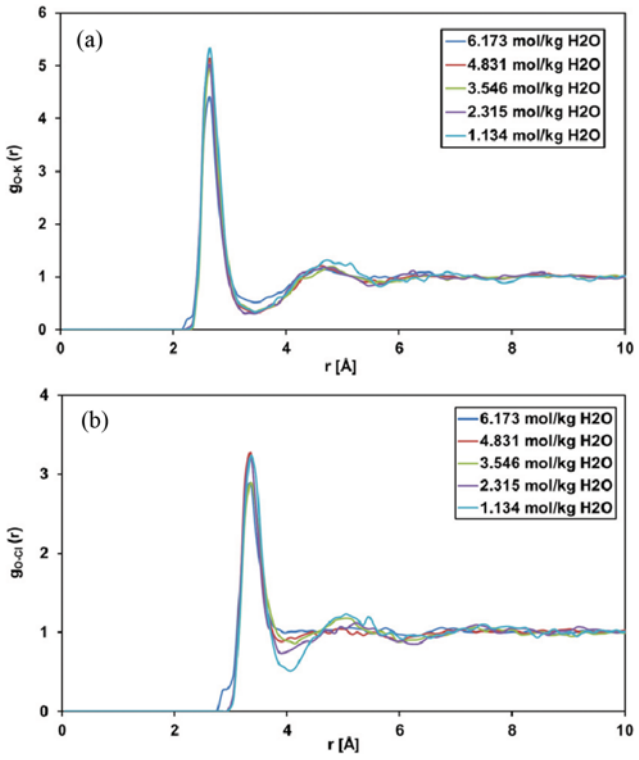

Fig. 7. Some RDFs of ion-water type at 300 K in various concentrations. (a) O-K and (b) O-Cl.

decreases. To investigate this issue, the hydration number of ions should be determined. The hydration number of ions in aqueous solution can be determined by the following equation [45]:

$$n_i = 4\pi\rho_{H_2O}\int_0^{r_{min}} r^2 g_{i,H_2O}(r)dr \quad (8)$$

where ρ_{H_2O} is the number density of water molecules and r_{min} denotes that integration must be performed up to the first minimum of the RDF. In the present work, the hydration numbers of potassium ions at 300 K for several concentrations were calculated and compared with the data reported by Mancinelli et al. [46]. The results are shown in Fig. 8. According to Fig. 8, as the potassium

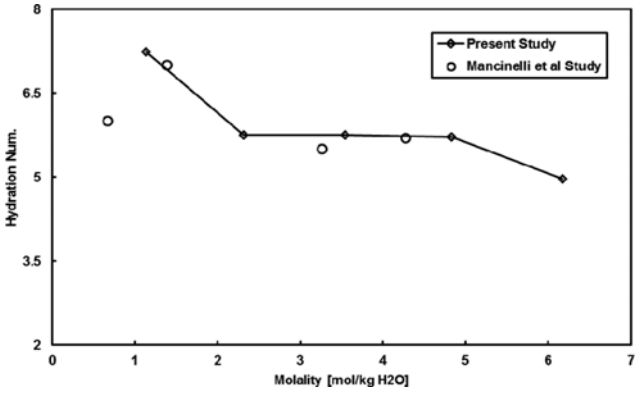

Fig. 8. A comparison between the hydration numbers of potassium ions in the present work and another study [46].

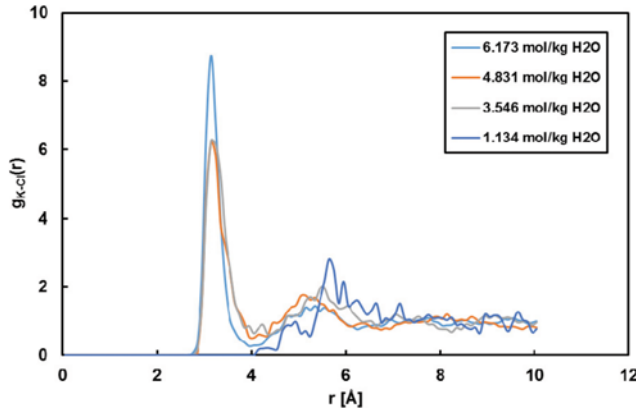

Fig. 9. The RDFs between potassium and chloride ions at 300 K for several ion concentrations.

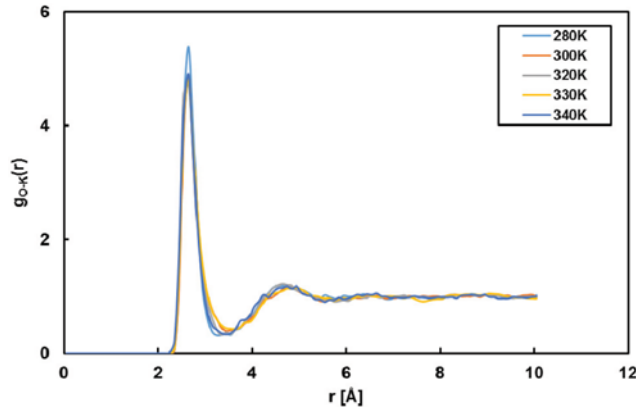

Fig. 10. The RDF between potassium ions and oxygen atoms for several temperatures with concentration equal to 3.546 mol/kg H_2O.

ion concentration in an aqueous solution increases, the hydration number of the ions decreases because at high concentration of ions, the number of ion pairs increases [47]. Thus, the number of ion-oxygen pairs decreases and the first peak in the RDF of ion-oxygen decreases. Increasing the number of ion pairs leads to increase in the first peak in the RDF of ion-ion. This fact is shown in Fig. 9.

Fig. 10 shows the RDFs between potassium ions and oxygen atoms in several temperatures for an aqueous KCl solution with molality equals to 3.546 mol/kg H_2O. According to this figure, when the temperature of the solution increases, the value of the first peak of RDF decreases. To investigate this issue, the local number density of water molecules near the potassium ion should be considered. Local number density of water molecules near the potassium ion is shown in Fig. 11. In Fig. 10, the distance of the first peak in the RDF is equal to 2.65 Å. According to Fig. 11, when the distance between water molecules and potassium ion is 2.65 Å, it seems that as the temperature of solutions increases, the local number density of water molecules approximately decreases. This is due to increment of kinetic energies of water molecules and ions. As the temperature of the aqueous ionic solution increases, the velocity of water molecules and ions grows and the solution expands. Because molecules and ions move faster than previous state, the residence

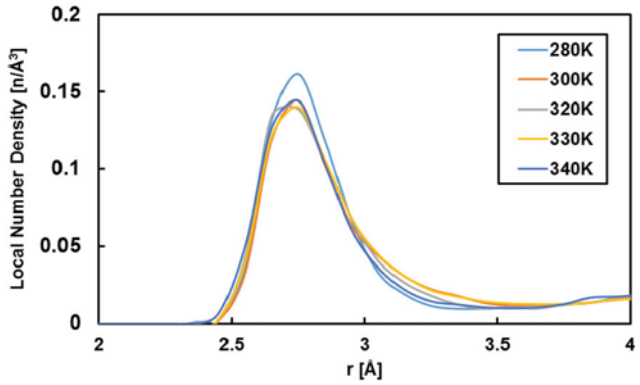

Fig. 11. Local number density of water molecules near the potassium ion.

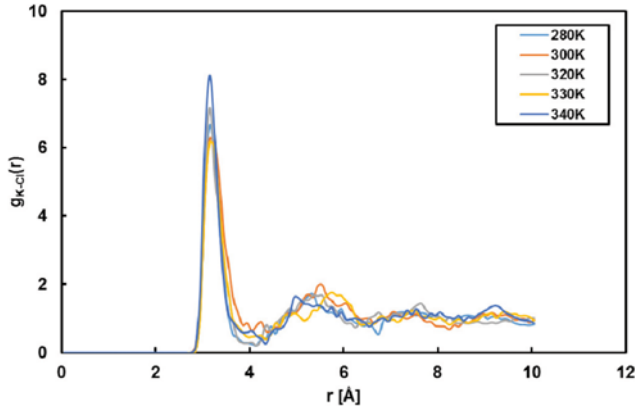

Fig. 12. The RDF between potassium and chloride ions for several temperatures at ion molality equal to 3.546 mol/kg H_2O.

time of water molecules in the hydration layer of the ions decreases and thus the density of water molecules around the ions is decreased. Fig. 12 shows the RDF between potassium and chloride ions for several temperatures. According to this figure, when the temperature increases, the first peak of the RDF grows. At higher temperatures, the molecules and ions move faster, the number of ion pairs grows and the first peak of the RDF moves up.

Fig. 13 shows the RDF between atoms of water molecules. In Fig. 13(a), as the concentration of the ions in aqueous ionic solution increases, the first peak of the RDF does not change, but it seems that the second peak moves downward. The first peak in $g_{O\text{-}H}(r)$ shows the covalent bonds between oxygen and hydrogen atoms in water molecules and they do not change during the simulation due to applying SHAKE algorithm. But the second peak shows the direct contact of oxygen and hydrogen of different molecules. As the concentration of ions in the solution increases, the number of oxygen-hydrogen pairs slightly decreases, and this leads to decreasing the value of the second peak of $g_{O\text{-}H}(r)$. The first peak of RDF in Fig. 13(b) is also decreased as the ion concentration increases. This can be attributed to the reduction of the number of oxygen-oxygen pairs as the ion concentration increases.

3. Self-diffusion Coefficients

According to section 2.1, in these simulations, the Einstein method is used to calculate self-diffusion coefficients. Thus, the sim-

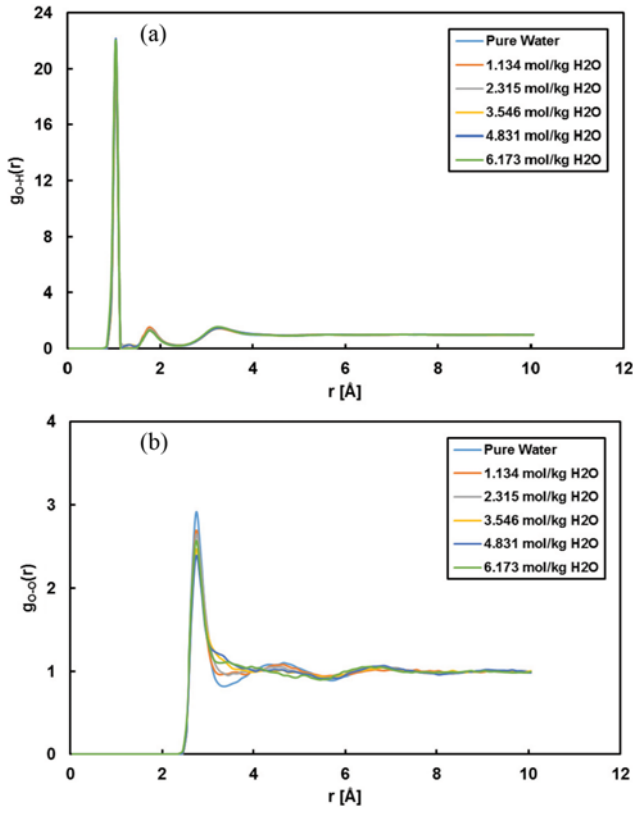

Fig. 13. The RDF between atoms of water molecules at 300 K. (a) oxygen-hydrogen and (b) oxygen-oxygen.

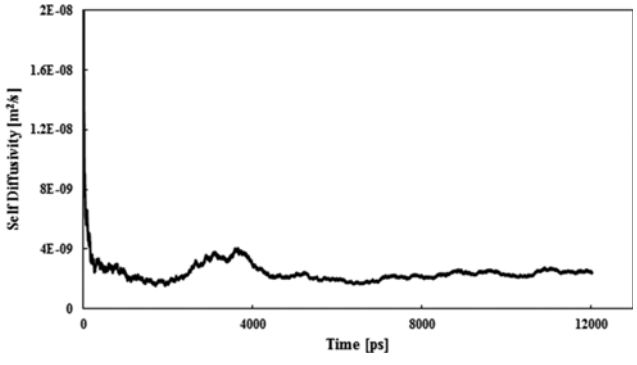

Fig. 14. Variation of self-diffusion coefficient during the simulation time.

ulations were performed for a large period of time (about 12 ns). The results of self-diffusion coefficient for one simulation during the time are shown in Fig. 14. From this figure, the self-diffusion coefficient converges to a constant value after passing approximately 5 ns. Self-diffusion coefficients were calculated directly by LAMMPS simulator. The values of self-diffusion coefficients for all simulations are shown in Tables 5 and 6. The self-diffusion coefficients of ions increase by an increase in the temperature and decrease by an increase in the ion concentration. But some of exceptions are present in the results.

Fig. 15 shows the difference between the self-diffusion coefficients of potassium and chloride ions based on Deublein force field.

Table 5. Values of self-diffusion coefficients in for all temperatures and concentrations. The Dang force field is used for interatomic potential of ions. Self-diffusion unit is (10^{-9} m^2/s)

Ion molality (mol/kg H_2O)		6.173	4.831	3.546	2.315	1.134
K^+	T=280 K	0.476	0.933	0.895	1.173	0.980
	T=300 K	0.808	0.988	1.215	1.624	1.878
	T=320 K	1.206	1.192	1.888	2.371	2.478
	T=330 K	1.414	1.723	2.064	3.004	2.635
	T=340 K	1.783	2.191	2.483	2.391	2.451
Cl^-	T=280 K	0.619	0.709	0.753	0.958	0.622
	T=300 K	0.982	1.019	0.915	1.525	1.381
	T=320 K	1.295	1.382	1.392	1.880	1.182
	T=330 K	1.752	1.704	1.852	1.976	1.535
	T=340 K	1.754	1.992	2.208	3.227	3.346

Table 6. Values of self-diffusion coefficients for all temperatures and concentrations. The Deublein force field is used for interatomic potential of ions. Self-diffusion unit is (10^{-9} m^2/s)

Ion molality (mol/kg H_2O)		6.173	4.831	3.546	2.315	1.134
K^+	T=280 K	0.551	0.639	0.654	0.880	1.133
	T=300 K	0.879	1.019	1.165	1.024	1.298
	T=320 K	1.054	1.473	1.870	1.920	2.329
	T=330 K	1.343	1.576	1.741	1.955	2.551
	T=340 K	1.523	1.886	2.096	2.225	2.643
Cl^-	T=280 K	0.454	0.614	0.585	0.919	0.816
	T=300 K	0.664	0.902	1.240	1.841	1.714
	T=320 K	1.482	1.274	1.419	1.682	2.302
	T=330 K	1.489	1.343	1.680	2.659	1.999
	T=340 K	1.517	2.166	2.155	1.543	2.677

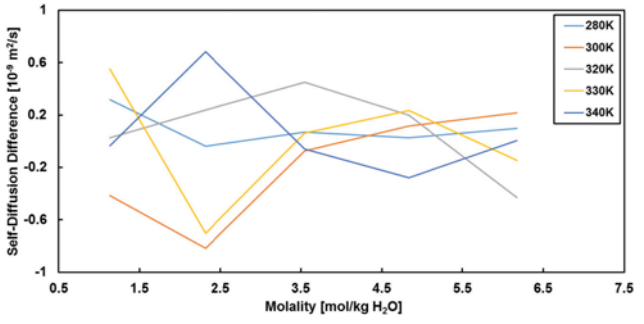

Fig. 15. The difference between self-diffusion coefficients of potassium and chloride ions for several temperatures based on Deublein force field.

This difference shows the difference between mobility of ions. It seems that at low temperature or high ion concentration the difference between the self-diffusion coefficients is small. Because the difference between the molecular weight of potassium and chlorine atoms is small, the effect of their masses on the mobility of ions can be neglected. Thus, for investigating the difference between

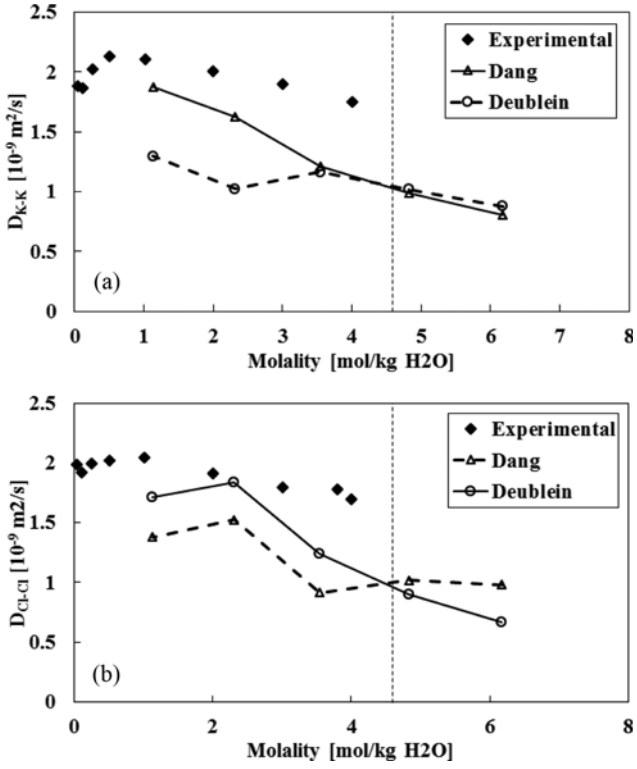

Fig. 16. Comparison between simulation results of self-diffusion coefficient and reported data at 300 K: (a) Potassium ion and (b) chloride ion.

self-diffusion coefficients, the effect of inter-atomic interactions should be considered. At low temperature or high concentration, the number of ion-ion pairs changes, and it can affect the difference of self-diffusion coefficients. For example, when the temperature of the aqueous solution decreases, the mobility of atoms and ions decreases and then the number of ion-ion pairs becomes smaller.

4. Validation of the Simulations

In this section, the results of present simulation are compared with the experimental results which were reported in refs. [35,48,49]. In these references, there are experimental data of the self-diffusion coefficients of aqueous KCl solution. The comparison of the present simulation results and the experimental reported data at 300 K is shown in Fig. 16. At low concentrations of Cl^-, which means low concentration of K^+ (equal or less than 3 mol/kg H_2O), the self-diffusion coefficients of potassium and chloride ions are predicted well by Dang and Deublein force fields, respectively. The relative error of each model from experimental data is calculated (see Fig. 17). At high concentration range, none of the above force fields can predict the experimental data accurately and both force fields have considerable deviations from the experimental data. In both Figs. 16(a) and 16(b), the dashed lines indicate the saturated aqueous solution of KCl for which its molality equals to 4.56 mol/kg H_2O.

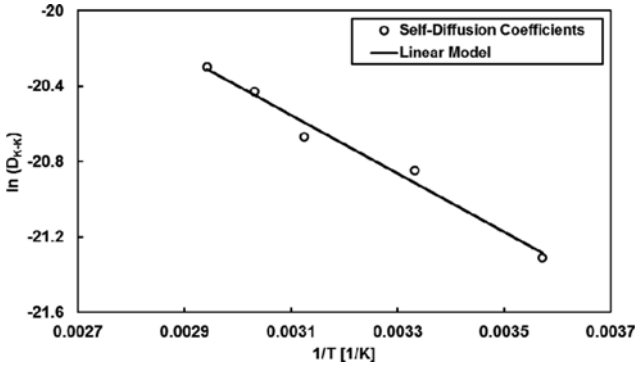

Fig. 18. Linear fitting the self-diffusion coefficient data. The ion concentration of all data is 6.173 mol/kg H_2O, The Deublein force field is used.

There is a large deviation of simulation results from experimental data at high concentration range, which may depend on the force fields used in the simulation. The force fields of water and ions may fail in the high concentration range. Thus, repetition of simulations with several force fields of water and ions reveals the effect of force fields on the final results. On the other hand, there are only a few experimental studies on the aqueous KCl solutions. In the case of availability of sufficient experimental studies at the same condition, the comparison of simulation results with experimental data will be more accurate.

5. Modeling the Temperature Effect

As mentioned earlier, the temperature effect on the self-diffusion coefficient can be modeled by an Arrhenius type equation. If the natural logarithm of the self-diffusion coefficients is plotted versus inverse of temperature and a linear curve is achieved, this effect can be modeled by Arrhenius type equation. An example of this plot is shown in Fig. 18. In this figure the natural logarithm of diffusion coefficients of K^+ with molality of 6.173 mol/kg H_2O is plotted versus 1/T. Eq. (9) shows the variation of self-diffusion coefficient,

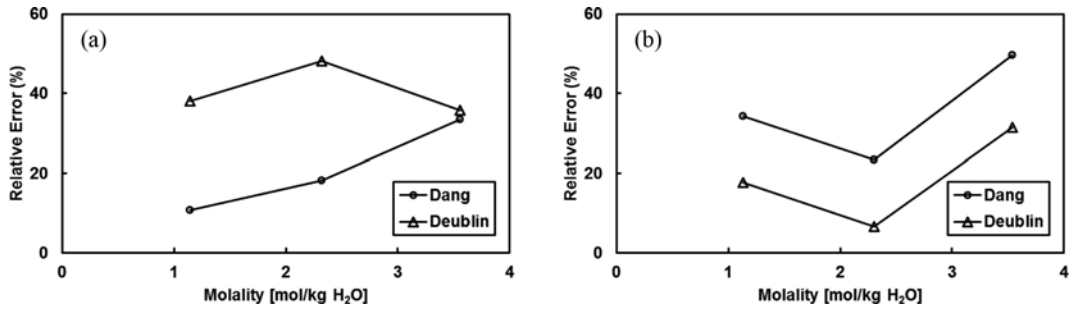

Fig. 17. Relative Errors of predicted self-diffusion coefficient of ions by Dang and Deublein models at 300 K. (a) K^+ and (b) Cl^-.

Table 7. The values of D_0 and E in for different ion concentrations based on Deublein force field

Molality of ion	K^+		Cl^-	
	$D_0\times10^7$ (m^2/s)	E (J/mol)	$D_0\times10^7$ (m^2/s)	E (J/mol)
6.173	1.49	12979.82	9.74833	17873.44
4.831	2.75	14049.83	3.68804	14981
3.546	4.85	15207.14	5.36071	15641.96
1.134	2.51	12722.91	4.18747	14204.47

which is plotted in Fig. 18. According to Eq. (9) the slope of this plot shows the diffusion activation energy. Table 7 contains the values for D_0 and diffusion activation energy (E) for different concentration of K^+ and Cl^- ions.

$$D_{K-K}=1.49\times10^{-7}\exp\left(-\frac{12813.54}{RT}\right) \quad (9)$$

CONCLUSION

Fifty MD simulations were performed for aqueous KCl solutions with two different force fields of ions. The performance of two force fields was investigated by prediction of the self-diffusion coefficients of K^+ and Cl^- at various temperatures and ion concentrations. Also, the temperature effect was modeled by Arrhenius type equation. Each simulation was performed for long enough time (about 12 ns) to achieve accurate self-diffusion coefficients. The effect of temperature on the RDFs was discussed in detail at different temperatures and ion concentrations.

It was found that at low concentrations, the Dang and Deublein force fields can be used to predict the self-diffusion coefficients of potassium and chloride ions, respectively. At high concentration range, predicted data by both force fields approach each other, but the deviation from experimental data was considerable. Furthermore, using an Arrhenius type equation, diffusion activation energies at different ion concentrations were calculated.

REFERENCES

1. A. Ghaffari and A. Rahabar-Kelishami, *J. Mol. Liq*., **187**, 238 (2013).
2. R. Parthasarathi, J. Sun, T. Dutta, N. Sun, S. Pattathil, N. V. S. N. Murthy Konda, A. G. Peralta, B. A. Simmons and S. Singh, *Biotechnol. Biofuels*, **9**, 1 (2016).
3. A. A. Chilavo and L. Vlcek, *Fluid Phase Equilib*., **407**, 84 (2015).
4. H. Y. Lee, V. Manivannan and J. Goodenough, *C.R. Acad. Sci., Ser. IIc: Chim*., **2**, 565 (1999).
5. I. Edelman and J. Leibman, *Am. J. Med*., **27**, 256 (1959).
6. G. Shekhtar, M. Rai, N. P. Mahulkar and P. B. Karandikar, in Electronics and Communication Systems (ICECS), 2nd International Conference on, Coimbatore (2015).
7. M. Kim, l. Oh and J. Kim, *Phys. Chem. Chem. Phys*., **17**, 16367 (2015).
8. M. H. Rausch, L. Hopf, A. Heller, A. Leipertz and A. P. Fröba, *J. Phys. Chem. B*, **117**, 2429 (2013).
9. L. Syam Sundar, E. Venkata Ramana, M. K. Singh and A. C. M. Sousa, *Int. Commun. Heat Mass Transf*., **56**, 86 (2014).
10. D. I. Sagdeev, M. G. Fomina, G. K. Mukhamedzyanov and I. M. Abdulagatov, *Int. J. Thermophys*., **34**, 1 (2013).
11. B. K. Dutta, Principle of Mass Transfer and Separation Process, PHI Learning Pvt. Ltd., New Dehli (2009).
12. T. K. Sherwood, R. L. Pigford and C. R. Wilke, Mass Transfer, McGraw-Hill (1975).
13. R. Kimmich, W. Unrath, G. Schnur and E. Rommel, *J. Magn. Reson*., **91**, 136 (1991).
14. A. Meyer, *Phys. Rev. B*, **81**, 1 (2010).
15. J. Lascombe, Molecular Motions in Liquids: Proceedings of the 24th Annual Meeting of the Société de Chimie Physique Paris-Orsay, 2-6 July 1972, Springer Science & Business Media (2012).
16. A. Anderko and M. M. Lencka, *Ind. Eng. Chem. Res*., **37**, 2878 (1998).
17. P. Wang and A. Anderko, *Ind. Eng. Chem. Res*., **42**, 3495 (2003).
18. Z. Chenyu, Y. K. Shin, A. C. T. van Duin, H. Fang and Z.-K. Liu, *Acta Mater*., **83**, 102 (2015).
19. N. Zhang, Z. Shen, C. Chen, G. He and C. Hao, *J. Mol. Liq*., **203**, 90 (2015).
20. F. Landuzzi, L. Pasquini, S. Giusepponi, M. Celino, A. Montone, P. L. Palla and F. Cleri, *J. Mater. Sci*., **50**, 2502 (2015).
21. J. N. Israelachvili, Intermolecular and Surface Forces, Elsevier Science (2015).
22. Z. Li, O. Borodin, G. D. Smith and D. Bedrov, *J. Phys. Chem. B*, **119**, 3085 (2015).
23. K. Xu, X. Ji, C. Chen, H. Wan, L. Miao and J. Jiang, *Electrochim. Acta*, **166**, 142 (2015).
24. N. N. Rajput, X. Qu, N. Sa, A. K. Burrell and K. A. Perrson, *J. Am. Chem. Soc*., **137**, 3411 (2015).
25. H. Kasemägi, M. Ollikainen, D. Brandell and A. Abloo, *Electrochim. Acta*, **175**, 47 (2015).
26. M. Duvail, A. Villard, T.-N. Nguyen and J.-F. Dufrêche, *J. Phys. Chem. B*, **119**, 11184 (2015).
27. K. Meier, A. Laesecke and S. Kabelac, *Int. J. Thermophys*., **22**, 161 (2001).
28. F. A. Furtado, C. R. A. Abreu and F. W. Tavares, *AIChE J*., **61**, 2881 (2015).
29. G. Guevara-Carrion, C. Nieto-Draghi, J. Vrabec and H. Hasse, *J. Phys. Chem. B*, **112**, 16664 (2008).
30. L. Wei-Zhong, C. Cong and Y. Jian, *Heat Tran. Asian Res*., **37**, 86 (2008).
31. L. X. Dang and B. M. Pettitt, *J. Phys. Chem*., **91**, 3349 (1987).
32. H. Berendsen, J. Grigera and T. Straatsma, *J. Phys. Chem*., **91**, 6269 (1987).
33. W. Jorgensen, J. Chandrasekhar, J. Madura, R. Impey and M. Klein, *J. Chem. Phys*., **79**, 926 (1983).

34. W. L. Jorgensen and J. D. Madura, *Mol. Phys*., **56**, 1381 (1985).
35. J. O. Sindt, A. J. Alexander and P. J. Camp, *J. Phys. Chem. B*, **118**, 9404 (2014).
36. S. Deublein, J. Vrabec and H. Hasse, *J. Chem. Phys*., **136**, 1 (2012).
37. T. Schnabel, Molecular Modeling and Simulation of Hydrogen Bonding Pure Fluids and Mixtures, Logos Verlag, Berlin (2008).
38. P. Mark and L. Nilsson, *J. Phys. Chem. A*, **105**, 9954 (2001).
39. M. P. Allen and D. J. Tildesley, Computer Simulation of Liquids, Clarendon Press (1989).
40. R. Zhou, Molecular Modeling at the Atomic Scale: Methods and Applications in Quantitative Biology, CRC Press, NewYork (2014).
41. S. Plimpton, *J. Comput. Phys*., **117**, 1 (1995).
42. J. M. Seminario, Design and Applications of Nanomaterials for Sensors, Springer Netherlands (2014).
43. S. Al Ghafri, G. C. Maitland and J. Trusler, *Chem. Eng. Data*, **57**, 1288 (2012).
44. D. Tabor, Gases, Liquids and Solids: And Other States of Matter, Cambridge University Press, Cambridge (1991).
45. R. Catlow, S. C. Parker and M. P. Allen, Computer Modelling of Fluids Polymers and Solids, Springer Netherlands (2012).
46. R. Mancinelli, A. Botti, F. Bruni, M. A. Ricci and A. K. Soper, *J. Phys. Chem. B*, **111**, 13570 (2007).
47. S. Chowdhuri and A. Chandra, *J. Chem. Phys*., **115**, 3732 (2001).
48. A. M. Friedman and J. W. Kennedy, *J. Am. Chem. Soc*., **77**, 4499 (1955).
49. R. Mills, *J. Phys. Chem*., **61**, 1631 (1957).